ER-3602

RELATIONSHIP BETWEEN SHEAR WAVE BIREFRINGENCE AND FRACTURE SPACING: A LABORATORY STUDY

by

Khalid Al-Mashouq

ER-3602

An Engineering Report is submitted to the Faculty and the Board of Trustees of the Colorado School of Mines in partial fulfillment of the requirements for the degree of Master of Engineering (Geophysical Engineer).

Golden, Colorado

Date 11/9/1988

Signed: Khalid Al-mashouq

Khalid Al-Mashouq

Approved: Abdelwahid Ibrahim

Abdelwahid Ibrahim
Thesis Advisor

Golden, Colorado

Date: 11/9/1988

P R Romig

Philip Romig, Chairman
Geophysics

ABSTRACT

A physical model study was initiated to observe shear-wave anisotropy in simulated fractured media. The study required the construction and calibration of shear-wave transducers, as well as the construction of the physical model. In a series of models, fracturing is simulated by stacks of thick plexiglass sheets clamped tightly together to form a block.

Observation of direct shear-wave arrivals through the stack, with propagation parallel to the plane of the sheets, definitely demonstrated the existence of anisotropy and shear-wave splitting. This was accomplished by allowing the polarization of the particle motion to be parallel to, normal to, or at any arbitrary angle to the plates.

For plexiglass sheets 1/16" thick, representing a fracture density of about 11 fractures per wavelength, strong anisotropy and shear-wave splitting are clearly observed. Observations for 1/4" sheets, about 3 fractures per wavelength, indicate that the anisotropy is more difficult to observe.

The results from the experimental relation between fracture intensity (expressed in fractures/inch) and the degree of anisotropy (expressed as a relative time delay)

which were observed as shear-wave splitting, suggest that the relation between fracturing and time delay appears to be linear.

When the three thicknesses (1/16", 1/8", and 1/4") are mixed to form a model, the degree of anisotropy for this model tends to be the average of the degree of anisotropies for the three models individually. This suggests that the real field data, the degree of observed anisotropy in the results reflects an average of the constituent anisotropies.

TABLE OF CONTENTS

LIST OF FIGURES

LIST OF TABLES

ACKNOWLEDGEMENTS

I would like to take this opportunity to thank the members of my committee, Dr. Abdelwahid Ibrahim, Dr. Guy Towle, and Dr. Ron Knoshaug for their continuous help during the course of my work. My advisor, Dr. Abdelwahid Ibrahim deserves special recognition for his valuable assistance and suggestions which proved tremendously helpful throughout this project.

INTRODUCTION

An anisotropic medium is one in which the physical properties governing elastic wave propagation vary with direction. The variation in these properties may result from crystalline anisotropy preferred mineral alignment, or fractures. Recent observations of seismic wave velocity anisotropy have been related to the study of fracturing in rocks. Both P-wave anisotropy, where P-wave velocity varies with direction of propagation, and S-wave anisotropy, where S-wave velocity varies with polarization, as well as propagation direction, have been observed in fractured rocks.

Recently, significant effort has been expended in both P-wave and S-wave anisotropy studies. Bamford and Nunn (1979) did measurements of P-wave velocity anisotropy in fractured carboniferous limestone. The cracked rocks contain either a naturally occurring preferred orientation of cracks (cracks caused by tectonic stress fields, temperature gradients, or recrystallization), or induced cracks with preferred orientation (the induced cracks orientation caused by the closure of the cracks results from the action of a nonhydrostatic stress on rocks which contain randomly orientated cracks). Their results suggest that by using relatively unsophisticated equipment, they were able

to measure large degrees of P-wave anisotropy (15-29%) which is well above the weak anisotropy (<10%) level.

Crampin (1980) studied P-wave anisotropy by interpreting the velocity measurements of Bamford and Nunn (1979). He calculated synthetic seismograms for P-wave propagation through cracked structures. His synthetic seismograms demonstrate polarization anomalies on three component records, which are diagnostic of propagation through cracked or anisotropic structures.

For the S-wave anistropy, much work has been done. For example, Johnston (1986) carried out a field experiment in Marcelina Creek field, Wilson County, Texas, which was designed to directly measure the effects of fracture-induced anisotropy on the propagation of seismic P- and S-waves. To measure velocity anisotropy, he used S-waves generated from a shear-wave vibrator on two seismic lines. The first line S-waves were propagated with polarization parallel and the second line S-waves were propagated with polarization perpendicular to the preferred fracture orientation as determined from borehole televiewer data. Also he completed two S-wave lines with polarizations 45 degrees to the fracture orientation. These two lines provided the optimal opportunity to detect S-wave splitting. His results suggest that S-wave velocity anisotropy may be observed from surface seismic data and recording both SH- and SV-waves was

necessary to evaluate subsurface fractures.

Becker and Perelberg (1986) investigated fracture-induced anisotropy using 3-component VSP data. From this data they were able to extract information about zones of anisotropy in the subsurface. Since subsurface fracturing is a cause of anisotropy, also they were able to identify zones of fracturing from the ellipticity information extracted using this data. They reported that detection of shear-wave splitting using 3-component VSP data can identify zones of anisotropy. Wave splitting can also indicate the principal axes directions and may give information regarding the degree of anisotropy. Also they reported that the degree of ellipticity, resulting from fracture-induced anisotropy, can be used to quantify the fracture density in an anisotropic zone.

Alford (1986) investigated the effects of azimuthal anisotropy on shear data acquired at Dilley, Texas. He reported that shear polarization splitting caused by azimuthal anisotropy can contribute to poor shear data quality. He indicated that if the incident polarization conforms to one of the preferred directions, e.g., either parallel or perpendicular to the principal axis of the azimuthally anisotropic medium, energy simply propagates at the appropriate velocity. And if the polarization of the

incident wave does not correspond to one of the preferred natural directions, motion of the incident wave is vectorally resolved along the natural axes and the situation becomes more complicated. He used a simple one-dimensional model. His model suggests that the sources and receivers of the acquisition system must be oriented to conform with the principal axes of the azimuthally anisotropic medium before a simple interpretation of the shear data is valid. He reported that many of the problems associated with shear waves in exploration may have been at least partially the result of neglecting the effects of shear wave propagation in an azimuthally anisotropic medium.

Laboratory studies on rock samples also give similar results on S-wave anisotropy. For example, Lo (1986) did measurements of P-, SH- and SV-wave velocities for three samples of rock (chelmsford granite, chicopee shale, and berea sandstone) as a function of direction. He also applied confining pressure on the sample to study the variation of anisotropy as a function of confining pressure. His result suggests that anisotropy in these rocks is primarily due to the preferred orientation of (1) constituent minerals which are generally anisotropic; (2) textural-structural features like bedding or foliation; and (3) pores and cracks. He also reported that the effects due

to cracks and pores should decrease with increasing confining pressure because of the closing of cracks. He also mentioned that the dominant cause of anisotropy at high confining pressures are the preferred mineral orientation and the compositional stratification.

Another example of study is by Rai (1986). His study was on the measurement of shear-wave birefringence as a function of both hydrostatic and uniaxial stress in sedimentary rocks. The samples which were included in the study were sandstones, limestones, and shales. For the hydrostatic stress experiments, he mounted piezoelectric shear wave transducers on the sample in such a way that the polarization direction of the receiver transducer was orthogonal to the polarization direction of the transmitter. With this kind of arrangement of transducers, shear-wave signals are received only when the rock sample is azimuthally anisotropic. For the uniaxial stress experiments, the arrangement of transducers was such that two shear-waves were propagated normal to the stress direction, one with polarization parallel and the other with polarization perpendicular to the direction of the uniaxial stress. He found out that the amplitude of the received signal is strongly dependent on the pressure. It decreases with increasing pressure. Around 2300 psi, the received

signal amplitude becomes negligible for the sandstone sample. So with increasing pressure the sandstones become less and less anisotropic. The reason for that is the crack's closure; therefore the hydrostatic stress was found to diminish birefringence in the samples.

For the uniaxial stress experiment, he reported that sandstone shows increasing birefringence with uniaxial stress, whereas the limestones show relatively little birefringence, and the shale sample shows no birefringence at all. From these observations one may conclude that of the three rock types tested, the sandstones probably have the greatest density of microcracks.

Results of field experiments and laboratory studies suggest that velocity anisotropy of seismic waves could potentially evolve into a technique of seismically detecting zones of oriented fractures in the subsurface. Because of the difficulty of knowing the fracture intensity in the field, a physical model experiment was conducted which allowed the study of shear-wave splitting. In this experiment, anisotropy and fracture intensity for fractured media were studied.

The experimental work required the construction and calibration of shear wave transducers and also the construction of the physical models.

THEORY

Anisotropic media are any media whose properties vary with direction. Wave motion in an anisotropic solid is fundamentally different from motion in an isotropic solid. Seismic waves penetrating such anisotropic material display a number of characteristic and diagnostic properties, which are subtly different from those of waves propagating in isotropic solids. The elastic behavior of an anisotropic medium with respect to appropriate seismic wavelengths can be described by effective elastic constants in one of a range of anisotropic symmetry systems. Uniform homogeneous elastic solids may be divided into eight anisotropic symmetry systems with distinct and individual properties. These eight systems include, the isotropic system with maximum symmetry where every plane is a symmetry plane, and the triclinic system with minimum symmetry where there are no symmetry planes (Crampin, 1981). In this paper, we desribe the physical behavior of wave motion required to understand and interpret observations of wave propagation in anisotropic solids.

Background

There are some basic relationships which can be found in any textbook of theoretical elasticity (for example,

Love, 1944). These relationships will be used here without a proof. They do provide the essential mathematical background on which the understanding of wave propagation in anisotropic media is based.

(1) The equations of motion for wave propagation with infinitesimal displacements in a purely anisotropic medium in equilibrium are:

$$\rho \ddot{u}_j = C_{jkmn}\, u_{m,nk} \; ; \tag{1}$$

where ρ is the density; $\ddot{u}_j$ is the second time derivative of the displacement field, $\ddot{u}_j = \partial^2 u_j / \partial t^2$, $\{C_{jkmn}\}$ is the fourth-order tensor of elastic constants; and $u_{m,nk} = \partial^2 u_m / \partial x_n \partial x_k$. All suffixes take the value 1, 2, and 3, and the suffix summation convention, whereby if any suffix occurs twice it is put equal to 1, 2, and 3 in turn and the results summed.

(2) Hooke's stress-strain relationship in three-dimension form is:

$$\sigma_{jk} = C_{jkmn}\, u_{m,n} \; ; \tag{2}$$

where $\{\sigma_{jk}\}$ is the second-order stress tensor; and $u_{m,n} = \partial u_m / \partial x_n$. Note that the stress tensor is necessarily a symmetric matrix with three mutually orthogonal principal directions of stress.

(3) The fourth-order tensor of elastic constants must transform by the tensor transformation law:

$$C'_{jkmn} = X'_{j,p}X'_{k,q}X'_{m,r}X'_{n,s}C_{pqrs} \quad (3)$$

where $X'_{j,p} = \partial X'_j/\partial x_p$ are the direction cosines.

(4) The elastic tensor has the following symmetries:

$$C_{jkmn} = C_{kjmn} = C_{mnjk} \cdot \quad (4)$$

Equations (1) and (2) show that there are 3^4=81 elastic constants, using the symmetry conditions in (4) will reduce the elastic constants from 81 to 21 independent constants.

These elastic constants are usually written in the form of the symmetric matrix as seen in Figure 1.

Phase Velocities

The velocities of plane body-waves in anisotropic media are obtained by substituting the expressions for plane waves into the equations of motion (1) to yield three simultaneous equations in ρC^2, where C is the phase velocity. There are several ways to do this. The conventional method is to express the equation for velocity in a particular direction in terms of direction cosines with respect to a coordinate system fixed in the anisotropic solid. These lead to three Kelvin-Christoffel equations which can be solved easily for three distinct body-waves, which generally have three distinct velocities.

$$
\begin{array}{cccccc}
C_{1111} & C_{1122} & C_{1133} & C_{1123} & C_{1131} & C_{1112} \\
C_{2211} & C_{2222} & C_{2233} & C_{2223} & C_{2231} & C_{2212} \\
C_{3311} & C_{3322} & C_{3333} & C_{3323} & C_{3331} & C_{3312} \\
C_{2311} & C_{2322} & C_{2333} & C_{2323} & C_{2331} & C_{2312} \\
C_{3111} & C_{3122} & C_{3133} & C_{3123} & C_{3131} & C_{3112} \\
C_{1211} & C_{1222} & C_{1233} & C_{1223} & C_{1231} & C_{1212}
\end{array}
$$

Figure 1. Typical Representation of the Symmetric Fourth-order Tensor of Elastic Constants (after Crampin, 1984).

The preferred method is the one which was proposed by Crampin (1970). In this method the elastic tensor with element C_{jkmn} is rotated in one direction (say x_1-direction) by the tensor transformation law (equation 3). By doing so all the problems are reduced to propagation with apparent velocity C in the x_1-direction. This has advantages in that all analytical expressions and computer programs can be written in cosine general forms by making use of the summation convention for repeated suffixes.

A plane-wave propagating in the x_1-direction, with phase velocity C, can be written:

$$u_j = a_j \exp[iw(t-x_1/C)] \text{ for } j=1, 2, 3 . \qquad (5)$$

Substituting (5) into the equation of motion (1), we have three equations:

$$\begin{aligned} \rho C^2 a_1 &= C_{1111}a_1 + C_{1121}a_2 + C_{1131}a_3 \ ; \\ \rho C^2 a_2 &= C_{2111}a_1 + C_{2121}a_2 + C_{2131}a_3 \ ; \\ \rho C^2 a_3 &= C_{3111}a_1 + C_{3121}a_2 + C_{3131}a_3 \ . \end{aligned} \qquad (6)$$

The common multiplier $(iw)^2 \exp[iw(t-x_1/C)]$ is omitted.

These three equations can be solved in different ways. However, the preferred technique is to write the equations as linear eigenvalue problems for ρC^2, which can be solved by computer. We have:

$$(A - \rho C^2 I)\vec{a} = 0 \qquad (7)$$

where A is the 3x3 matrix with elements $\{C_{j_1k_1}\}$

$$A = \begin{pmatrix} C_{1111} & C_{1121} & C_{1131} \\ C_{2111} & C_{2121} & C_{2131} \\ C_{3111} & C_{3121} & C_{3131} \end{pmatrix} . \qquad (8)$$

I is the 3x3 identity matrix, and $\vec{a}$, with elements a_j, is the amplitude vector specifying the polarization of the particle motion. Since the matrix A is a real symmetric positive-definite submatrix of the full real symmetric positive-definite matrix of elastic constants from the tensor of elastic constants, the eigenvalue problem (7) has three real positive roots for ρC^2, with orthogonal eigenvectors $\vec{a}$. These equations immediately demonstrate some of the fundamental features of body-wave propagation in anisotropic media.

The three real roots of (7) show that there are three body-waves in every direction of phase propagation with orthogonal particle motion and with velocities which, in general, are different and vary with direction. These waves correspond to a quasi P-wave, qP, with approximately longitudinal particle polarization, and two quasi shear-waves, qSH and qSV, with approximately transverse particle motion. The term "quasi" is used because the compressional (P) is not purely dilatational; it includes some rotation while the two shear waves (SH and SV) are not purely rotational, they include some dilatation (Stonely, 1949).

Copley (1978) and Keith and Crampin (1977b) investigated wave propagation in anisotropic media. Both studies showed that for propagation directions off symmetry axes, all three body waves were affected. Copley (1978) noted that the particle motion of compressional waves was not purely longitudinal but contained components of both transverse modes. He also noted that the particle motions of the two shear modes, although orthogonal to the compressional wave motion, were not strictly horizontally and vertically polarized. Keith and Crampin (1977a) arrived at similar conclusions but also looked into reflection and transmission behavior at an isotropic-anisotropic boundary. They concluded that all three body waves were coupled in this mediuim. In other words, any incident waveform would give rise to a reflected and transmitted "P," "SV," and "SH" wave. This cross-coupling of all waveforms obviously results in extremely complicated reflection and transmission coefficients, especially for anisotropic media in contact.

Keith and Crampin (1977c) noted that in an anisotropic medium the two shear components were coupled, and their respective particle motion directions and velocities were controlled by the symmetry axes of the solid. This fact can be used to illustrate the added dimension shear-wave prospecting has over P-wave prospecting. Shear-wave

particle motion can be assumed to be normal to the propagation direction. Because of this, the velocity and reflection and transmission coefficients will depend not only on the propagation direction, but also on the particle motion direction.

A shear wave entering a region of anisotropy necessarily has to split into the two or more fixed polarizations along a particular direction of energy propagation. There will generally be a qP-wave component as well, but this is usually small, and can be neglected. These distinct shear waves (qSH and qSV) result in shear-wave splitting (also known as shear wave birefringence and shear-wave double-refraction). These fixed quasi shear-waves travel at different velocities and separate in time, so that on re-entry into an isotropic region, the original pulse cannot be reconstructed. Thus the passage through a region of anisotropy writes a characteristic signature into the polarization of the shear wave trains, which, because shear-waves have a unique velocity in isotropic media, is preserved for the remaining isotropic sections of the path. The phenomenon is illustrated schematically in Figure 2.

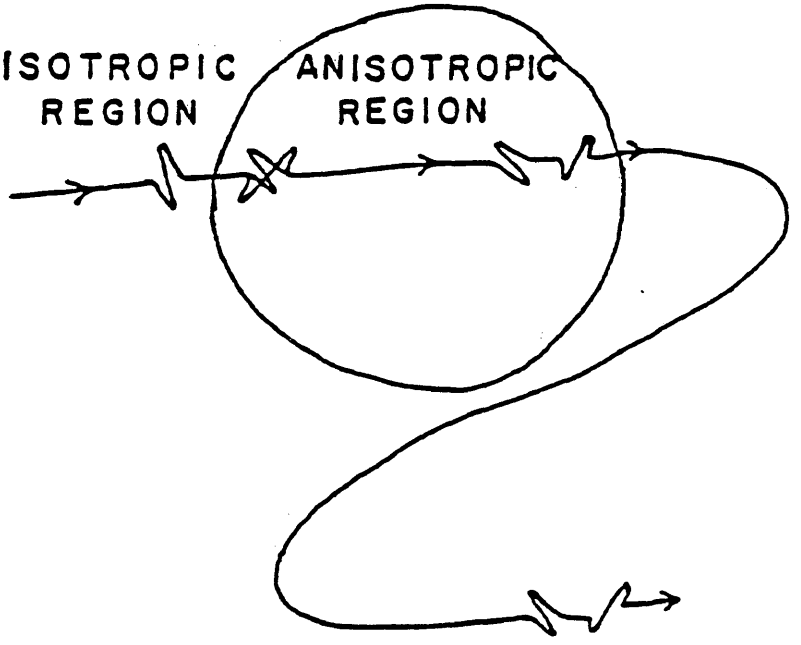

Figure 2. Schematic Illustration of Shear-wave Splitting (after Crampin, 1985).

A shear-wave entering an anisotropic region necessarily splits into the two or more fixed polarizations which can propagate in the particular ray direction. These split phases propagate with different polarizations and different velocities, and on re-entering an isotropic region the original wave form cannot be reconstructed.

LABORATORY STUDY

Instrumentation

The instruments which we used to conduct the experiment consist of:

a) HP pulse generator - model 214A. It gives maximum pulse amplitude of 100 volts, variable pulse width duration, repetition rate.

b) Oscilloscope to view the signal - Model 206 made by Nicolet Instrument Corporation with accuracy of 1 μs per point.

c) HP plotter to plot the signal from the oscilloscope.

d) Two shear-wave transducers.

Source and Receiver

Both source and receiver are shear-wave transducers (Pizeoelectric transducers, Vernitron PZT-A5). These transducers were sandwiched between two circular brass plates. Electric connection to the oscilloscope and the pulse source were accomplished through coaxial cable and conducted to the brass plates. A calibration test on the transducers was run to establish a clear accuracy of shear-wave polarization direction of the source. The calibration test was conducted as follows.

Both the source and the receiver were aligned together according to the marked arrows that are placed on the transducers by the manufacturer. These arrows indicate the polarization direction. The test was run on a solid block of plexiglass between the transducers. The position where the two arrows on the transducers was aligned was used as a reference orientation. The source then was held at a fixed position (the reference orientation), and the receiver then was rotated with incremental angles from the reference orientation.

The rotation of the receiver was done in the following manner.

First, the receiver was rotated clockwise from the reference orientation with 2.5 degree increments, until 5 degrees was reached. During these rotations, the amplitude of the received signals with incremental angles from the reference orientation was examined. From the received amplitudes, the reference orientation yielded the maximum sensitivity (highest amplitude). In both cases, pressure on the transducers was kept constant.

Another test was run on the transducers to determine the transit time of the seismic pulse in the transducers. The test was conducted as follows: the receiver was put on top of the source directly without any material between

them. The timing of the direct arrival of the shear-wave energy through the transducers was measured to be 1 microsecond (μs). This time will be subtracted from the shear-wave transit times through the samples to give the corrected shear-wave arrival times.

The Physical Models

Two types of models were constructed to conduct the experiment. Both types were constructed from thin plates of plexiglass. In Type I, a constant thickness of the plates within each model was used to assure consistent fracture density. There were three models of this type. The first model was constructed with thickness of 1/4" plates, the second one with thickness of 1/8", and the third one with thickness of 1/16". Type II was constructed with mixed thickness of plates (thickness is not constant within the model). The purpose of the second type is to simulate real earth models, because fractures in earth exist in different spatial frequencies.

Figure 3 shows a sketch of the model configuration. The solid blocks shown in the sketch outside the fractured portion are used to prevent the P-wave energy leaving the transducer laterally and reflecting from the edge of the model, from interfering with the direct-arrived shear-wave energy (Tatham, 1987).

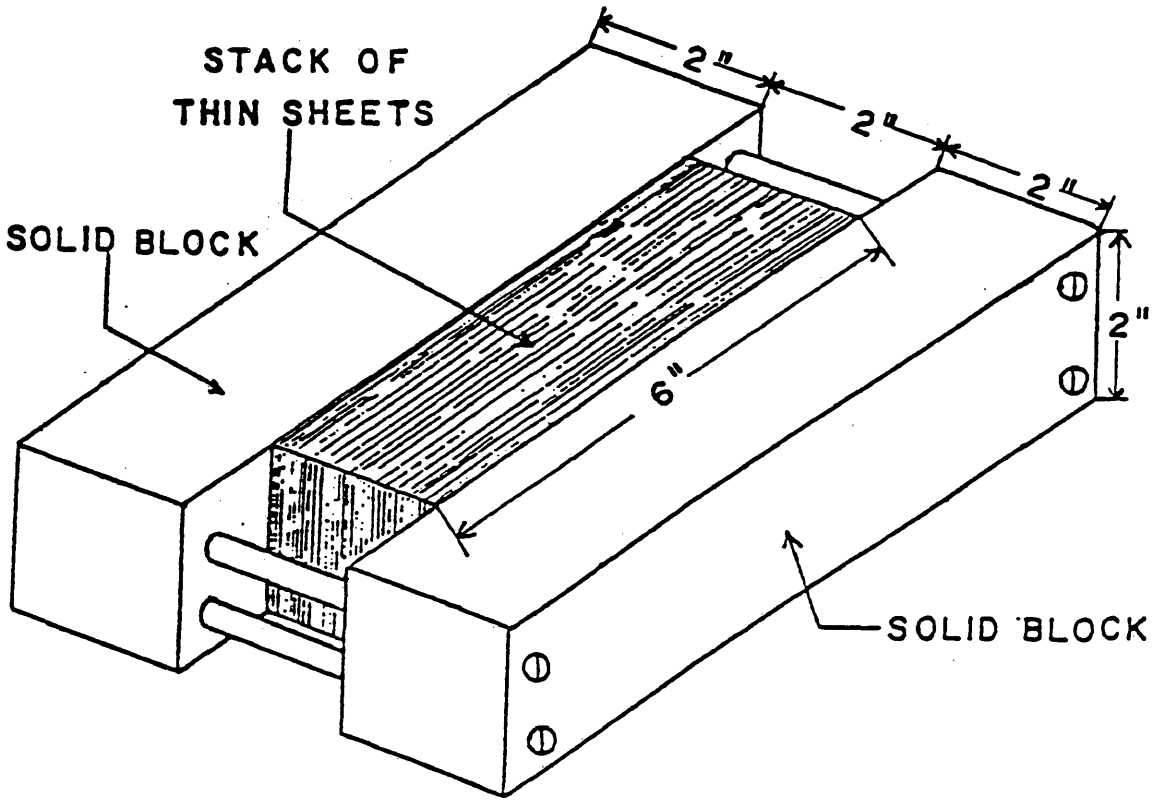

Figure 3. Schematic Drawing of One Model Simulating a Fractured Medium. Plexiglass Plates Represent Fractured Medium.

To ensure that the interfaces between the stack remain constant for different stacks, the models were assembled under the water, with a wetting agent (Photoflow) added to the water. The model was clamped together under the water leaving a thin film of water between the plates. The source was placed at the bottom of the model. The receiver was located vertically above the source, on the top of the model. This resulted in transmission of shear-wave energy directly through the model.

PROCEDURES AND RESULTS

For constant thickness plates, the tests were run on three models, with plate thicknesses of 1/16", 1/8", and 1/4" respectively. The test was conducted as follows.

The source and receiver polarization were aligned in such a way that the polarization of the particle motion was allowed to be parallel to the plates. This position is called zero (0) orientation. The source and receiver were rotated together in 10 degree increments in order to represent different polarization directions with respect to the orientation of the plates. When the polarization direction is perpendicular to the plates, this is called 90 degree orientation. The examination of the traces show the evidence of earlier arivals of the P-wave components. These arrivals appear as low amplitude before the onset of the shear-wave signals. The onset of the shear-wave signal was identified on the traces as a sudden downward deflection with high amplitude in relation to lower amplitude of the P-wave signals. Shear-wave velocity for the 0 degree was calculated to give $V_{\parallel}$, and shear-wave velocity for the 90 degree orientation to give $V_{\perp}$. The degree of shear-wave splitting was determined by taking the ratio of travel times (after subtracting the transit time in the transducers' assembly) for the 0 and 90 degree orientations.

Wavelength (λ) was calculated for each model to study the relationship between fracture density and shear-wave splitting. Wavelength (λ) was determined by dividing the velocity ($V_{\parallel}$) which was obtained from the transit time by the frequency of the received shear-wave signal which was obtained from the oscilloscope for each model.

The results from the three models are shown in Figures 4, 5, and 6. The shear-wave velocities ($V_{\parallel}$ - velocity of the 0 degree orientation) for 1/16", 1/8", and 1/4" thick plate models are 4008 ft/sec, 4244 ft/sec, and 4372 ft/sec, respectively. (See Tables 1, 2, and 3.)

The results in Figure 7 show a summary of anisotropy for the three models (1/16", 1/8", and 1/4"). This figure shows the relationship between the degree of anisotropy (the ratio of $V_{\parallel}/V_{\perp}$) and the crack density.

The results in Figure 8 show the traces for a model (Type II) with mixed thickness (thickness is not constant) of plates (I used 1/16", 1/8", and 1/4" thick plexiglass sheets). Shear-wave anisotropy here is not strong, but yet it is observed (the ratio of the travel times for the 0 and 90 degree orientations which gives us the degree of shear-wave splitting is about 1.199). The shear-wave velocity ($V_{\parallel}$ - the velocity of 0 degree orientation) for this model is about 4497 ft/sec (see Table 4).

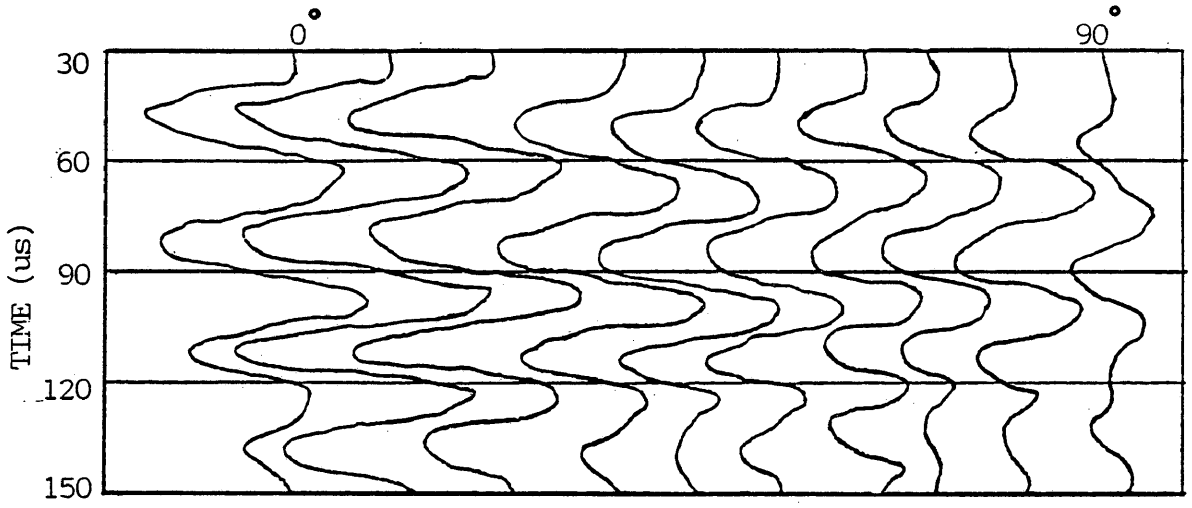

Figure 4. Shear Wave Arrivals Observed for 1/4" Plates. The traces shown here have the same propagation path, but different polarizations.

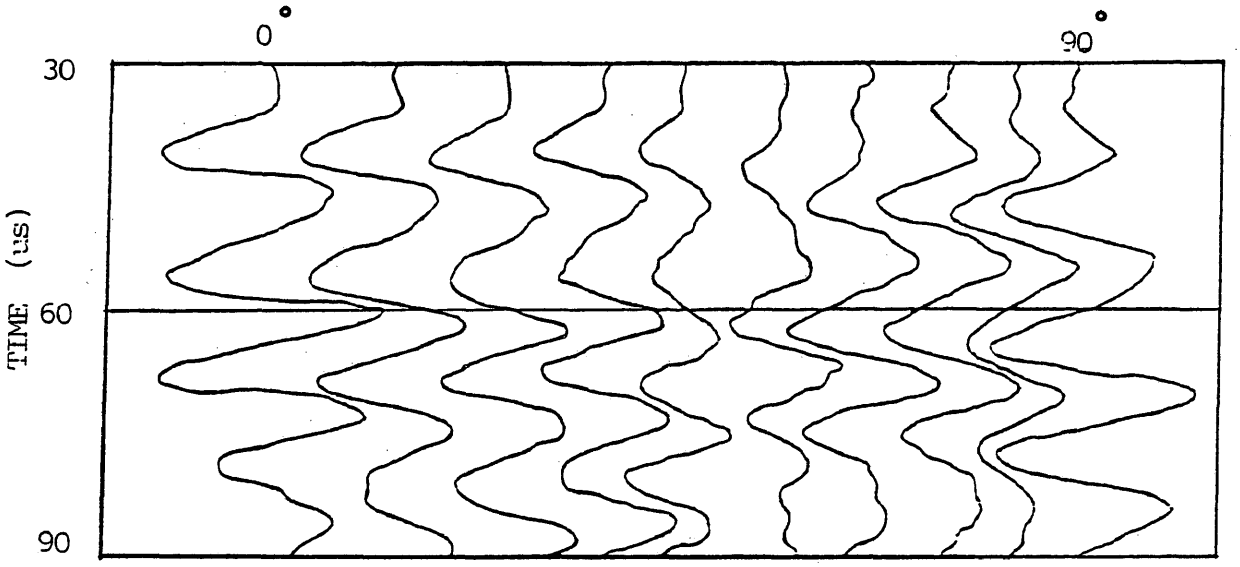

Figure 5. Shear-wave Arrivals Observed for 1/8" Plates.

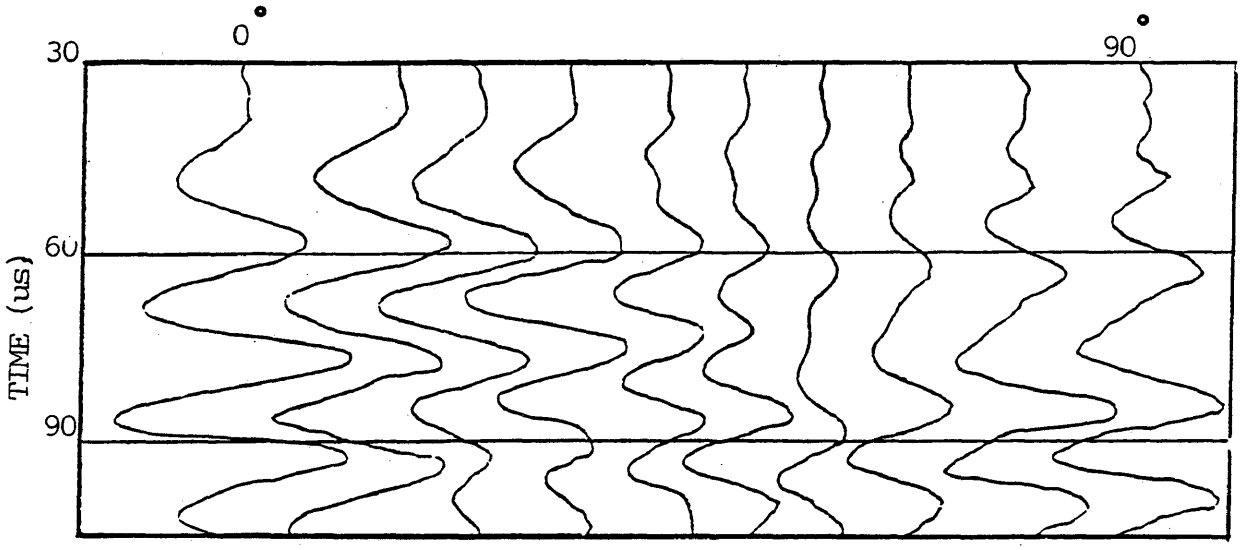

Figure 6. Shear-wave Arrivals Observed for 1/16" Plates.

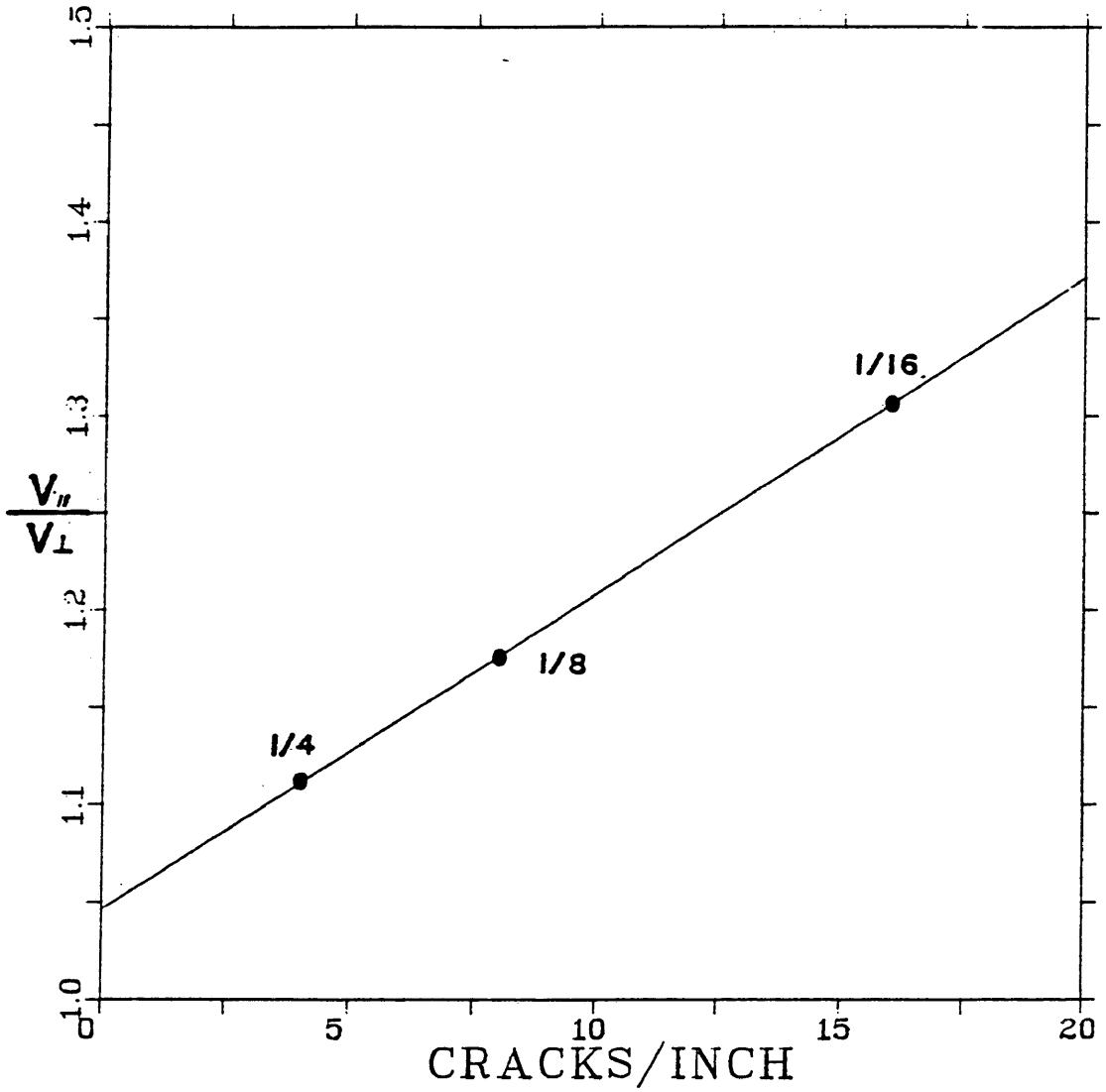

Figure 7. Summary of Anisotropy Observed from the Models.

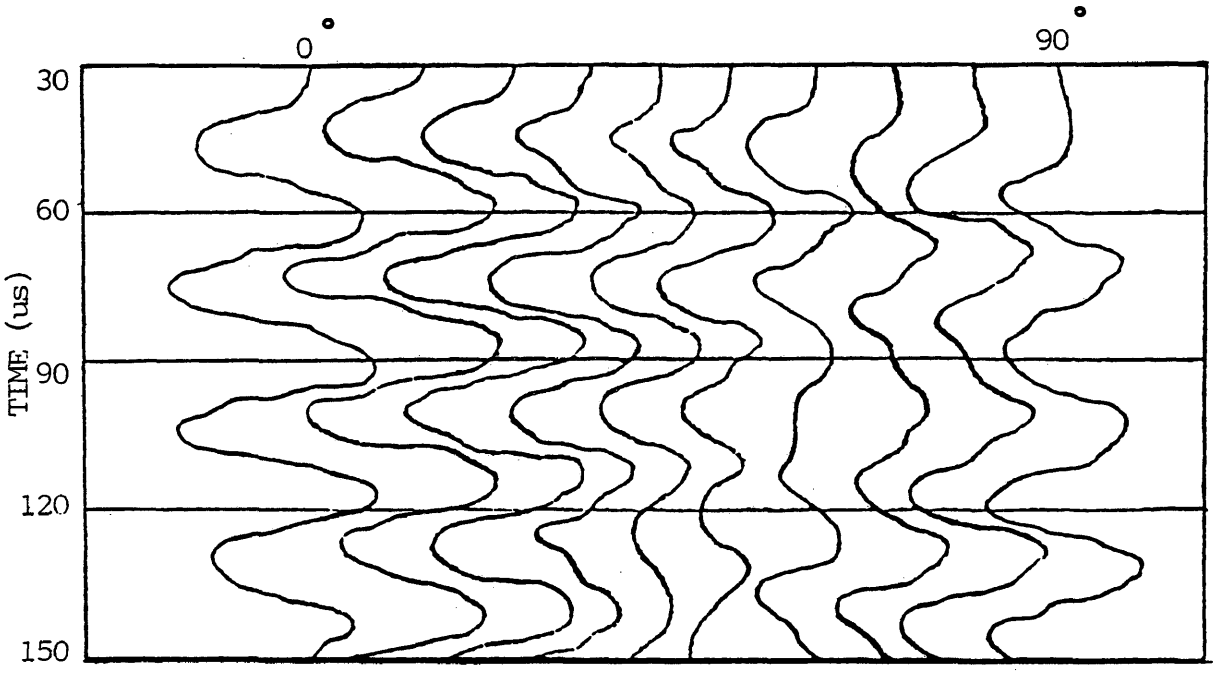

Figure 8. Shear-wave Arrivals Observed for the Mixed Model.

CONCLUSIONS

Shear-wave splitting, which was determined by taking the ratio of travel times (after correction for the transit time in the transducers) of the 0 and 90 degree orientations is observed for all models. Strong anisotropy and shear-wave splitting is clearly observed for the plexiglass sheets 1/16" thick model, and weak anisotropy is observed for the 1/4" thick plate model. From these results, we can conclude that as the fracture density increases, the degree of anisotropy (which gives shear-wave splitting) increases.

The relation between crack density and difference in shear-wave velocity with polarization exists. From the graph in Figure 7, which gives a summary of anisotropy for 1/16", 1/8", and 1/4" sheet models, we can conclude that the relation between fracture density and time delay appears to be a linear relationship. The R-squared value for the linear least square line is 0.999. For an isotropic material (zero cracks) the ratio of $v_{\parallel}/v_{\perp}$ equals one. From the figure, we can see that the best fit line does not intercept the value 1 for the ratio of $v_{\parallel}/v_{\perp}$. The author does not have a definite answer to this. A possible cause of this discrepancy might be the existence of another kind of anisotropy related to the make-up of the plexiglass plates.

When the three thicknesses are mixed to form a model, the ratio of the travel times which gives the degree of shear-wave splitting tends to be the average of the ratios of the three models. This suggests that in real field data, the degree of anisotropy observed in the results reflects an average of the constituent anisotropies.

Table 1. Shear-wave Velocities for 1/4" Plate Model.

Degree	Travel Time (TT) (in μs)	Velocity
0°	TT = 36	$V_{\parallel} = \frac{4.8}{36} \frac{cm}{\mu s} = 1333$ m/sec $= 4372$ ft/sec
90°	TT = 40	$V_{\perp} = \frac{4.8}{40} \frac{cm}{\mu s} = 1200$ m/sec $= 3936$ ft/sec
		Ratio of $\frac{V_{\parallel}}{V_{\perp}} = \frac{1333}{1200} = 1.111$

Period of the received shear signal = 15 μs

$$f = \frac{10^6}{15} = 66667 \text{ Hz}$$

$$\lambda = \frac{V}{f} = \frac{4372 \times 12}{66667} = 0.787"$$

Table 2. Shear-wave Velocities for 1/8" Plate Model

Degree	Travel time (TT) (in μs)	Velocity
0°	TT = 34	$V = \frac{4.4 \text{ cm}}{34 \ \mu s}$ = 1294 m/sec = 4244 ft/sec
90°	TT = 40	$V = \frac{4.4}{40} \frac{\text{cm}}{\mu s}$ = 1100 m/sec = 3608 ft/sec
		Ratio of $\frac{V_{\parallel}}{V_{\perp}} = \frac{1294}{1100} = 1.176$

Period = 14 μs

$f = \frac{10^6}{14} = 71428.5 \ H_z$

$\lambda = \frac{V}{f} = \frac{4244 \times 12}{71428.5} = 0.713"$

Table 3. Shear-wave Velocities for 1/16" Plates Model.

Degree	Travel Time (TT) = (in μs)	Velocity
0°	TT = 36	$V_{\parallel} = \frac{4.4}{36}\ \frac{cm}{\mu s} = 1222$ m/sec $= 4008$ ft/sec
90°	TT = 47	$V_{\perp} = \frac{4.4}{47}\ \frac{cm}{\mu s} = 936$ m/sec $= 3070$ ft/sec
		Ratio of $\frac{V_{\parallel}}{V_{\perp}} = \frac{1222}{936} = 1.306$

Period = 15 μs

$$f = \frac{10^6}{15} = 66667\ H_z$$

$$\lambda = \frac{v}{f} = \frac{4008 \times 12}{66667} = 0.721"$$

Table 4. Shear-wave Velocities for Mixed Thickness Model (mixed 1/16", 1/8", 1/4")

Degree	Travel Time (TT) = (in μs)	Velocities
0°	TT = 35	$V_{\parallel} = \frac{4.8}{35}\ \frac{cm}{\mu s} = 1371$ m/sec = 4497 ft/sec
90°	TT = 42	$V_{\perp} = \frac{4.8}{42}\ \frac{cm}{\mu s} = 1143$ m/sec = 3749 ft/sec
		$\text{Ratio} = \frac{V_{\parallel}}{V_{\perp}} = \frac{1371}{1143} = 1.199$

Period = 14 μs

$$f = \frac{10^6}{14} = 71428.5\ H_z$$

$$\lambda = \frac{V}{f} = \frac{4497 \times 12}{71428.5} = 0.755"$$

REFERENCES

Alford, R.M., 1986. Shear data in the presence of azimuthal anisotropy: Dilley, Texas: Presented at the 56th Annual SEG Meeting, Houston.

Bamford, D. and Nunn, K.R., 1979. In situ seismic measurements of crack anisotropy in the carboniferous limestone of Northwest England. Geophysical Prospecting, 27, 322-338.

Becker, D.F. and Perelberg, A. I. 1986. Seismic detection of subsurface fractures: Presented at the 56th Annual SEG Meeting, Houston.

Copley, J.H., 1978. Plane wave in an elastically anisotropic medium. Colorado School of Mines, Master's Thesis T-2043.

Crampin, S., 1970. The dispersion of surface waves in multilayered anisotropic media. Geophys. J.R. Astr. Soc., 21, 387-402.

Crampin, S., 1981. A review of wave motion in anisotropic and cracked elastic media, Wave Motion, 3, 343-391.

Crampin, S., 1984. An introduction to wave propagation in anisotropic media. Geophys. J.R. Astr. Soc., 76, 17-28.

Crampin, S., 1985. Evaluation of anisotropy by shear-wave splitting. Geophysics, 50, 142-152.

Crampin, S., McGonigle, R., and Bamford, D., 1980. Estimating crack parameters from observations of P-wave velocity anisotropy. Geophysics, 45, 345-360.

Crampin, S., Evans, R. and Atkinson, B.K., 1984b. Earthquake prediction: A new physical basis. Geophys. J.R. Astr. Soc., 76, 147-156.

Johnston, D.H., 1986. VSP detections of frature-induced velocity anisotropy. Presented at the 56th annual SEG meeting, Houston.

Keith, C.M., Campin, S., 1977a. Seismic body waves in anisotropic media: Reflection and refraction at a plane interface. Geophys. J.R. Astr. Soc., 49, 181-208.

_____ 1977b. Seismic body waves in anisotropic media: Propagation through a layer. Geophys. J.R. Astr. Soc., 49, 209-223.

_____ 1977c. Seismic body waves in anisotropic media: Synthetic seismograms. Geophys. J. R. Astr. Soc., 49, 225-243.

Lo, T.W., Coyner, K.B., and Toksoz, M.N., 1986. Experimental determinations of elastic anisotropy of Berea sandstone, Chicopee shale and Chelmsford Granite. Geophysics, 51, 164-171.

Love, A.E.H., 1944. A Treatise on the Mathematical Theory of Elasticity. 4th Ed., Dover, NY.

Rai, C.S. and Hanson, K.E., 1986. Shear-wave birefringence: A laboratory study. Presented at the 56th Annual SEG meeting, Houston.

Stonely, R., 1949. The seismological implications of aeolotropy in continental structure. Mon. Not. R. Astr. Soc. Geophys. Suppl., 5, 343-353.

Tatham, R.H., Matthews, M.D., Sekharan, K.K., and Wade, C.J., 1987. A physical model study of shear-wave splitting and fracture intensity: A laboratory study. Presented at the 57th Annual SEG meeting, New Orleans.